



# Subfreezing operation of polymer electrolyte fuel cells: Ice formation and cell performance loss

Jeffrey Mishler<sup>a</sup>, Yun Wang<sup>a,\*</sup>, Partha P. Mukherjee<sup>b</sup>, Rangachary Mukundan<sup>c</sup>, Rodney L. Borup<sup>c</sup>

<sup>a</sup> Renewable Energy Resources Lab (RERL), The University of California, Irvine, Irvine, CA 92697-3975, United States

<sup>b</sup> Texas A&M University, College Station, TX 77843, United States

<sup>c</sup> Los Alamos National Laboratory (LANL), Los Alamos, NM 87545, United States

## ARTICLE INFO

### Article history:

Received 10 November 2011

Received in revised form 6 January 2012

Accepted 7 January 2012

Available online 16 January 2012

### Keywords:

Subfreezing operation

Polymer electrolyte fuel cells

Neutron imaging

Experiment

Modeling

Analysis

## ABSTRACT

In this work, we investigate the cold-start operation of polymer electrolyte fuel cells (PEFCs) through high-resolution neutron radiography, experimental testing, theoretical evaluation, and comparison with model prediction. Ice formation location, voltage evolution, and loss of the electro-catalyst surface area (ECSA) are examined. A dimensionless parameter  $\bar{h}$ , characterizing the spatial variation of the reaction rate across the cathode catalyst layer, is discussed at subfreezing temperature using newly determined membrane ionic conductivity. The  $\bar{h}$  evaluation identifies the operating range that the reaction rate can be treated uniform across the catalyst layer, in which the model is valid.

© 2012 Elsevier Ltd. All rights reserved.

## 1. Introduction

The capability of polymer electrolyte fuel cells (PEFCs) to start up from subzero temperatures, also called cold start, is crucial to their transportation application. In subzero environments, water produced in electrodes freezes, resulting in reduced active electrochemical surface area and hindered reactant transport, see Fig. 1(a). The technical target set by the Department of Energy (DOE) for 2010 is the ability of the fuel cell stack to reach 50% rated power in 30 s starting from  $-20^{\circ}\text{C}$ , and the unassisted start-up temperature as low as  $-40^{\circ}\text{C}$  [1,2].

Cold-start experimental study has been attempted by several researchers [3–12]. Thompson et al. [7] used cryo-scanning electron microscopy to quantify the membrane water content, indicating that the membrane may absorb 14–15 water molecules per sulfonate group. Ge and Wang [8] presented a cyclic voltammetry (CV) study to investigate the effect of ice formation on the active catalyst area. Ishikawa et al. [9] investigated evidence of super-cooled water in the fuel cell, finding water freezing at the MEA/GDL interface. They expect that super-cooled water solidifies onto ice that remained after purging the fuel cell. Jiao et al. proposed different ice formation mechanisms for the cathode [10]. Jung and Um [11]

investigated the effect of a vanadium oxide film over the bipolar plate on non-isothermal cold start performance, indicating that the added thermal resistance enables more reaction heat to heat up the fuel cell and prevent cold-start failure. Hou et al. studied sequential cold-start at different current densities and explored degradation in cold-start ability for sequential failed cold starts [12].

Cold-start models have been created by different research groups [13–20]. Wang [13] analyzed the key parameters such as the time constants and obtained solutions to voltage loss due to ice formation and further compared their effects. Mao et al. [14] presented a cold-start model accounting for heat and water transport as well as ice formation. Wang et al. [16] defined three cold-start stages and experimentally determined the ionic conductivity at subfreezing temperatures. Voltage variation during nonisothermal cold start was also analyzed. Meng [17,18] investigated the impact of several parameters on isothermal cold-start behaviors and indicated that high gas flow rate, low initial membrane water content, low current density, and high cell voltage are beneficial to fuel cell cold start. Balliet and Newman [19] presented a two-dimensional cold start model which was used to study cold start for ultrathin cathode catalyst layers. Jiang et al. [20] developed a three-dimensional multiphase model of non-isothermal cold start, where the water and heat transport is numerically treated using the generalized transport equation [21]. Their simulation indicated that lumped thermal analysis may overestimate the amount of heat required to ensure successful fuel cell start-up.

\* Corresponding author. Tel.: +1 949 824 6004; fax: +1 949 824 8585.

E-mail address: [yunw@uci.edu](mailto:yunw@uci.edu) (Y. Wang).

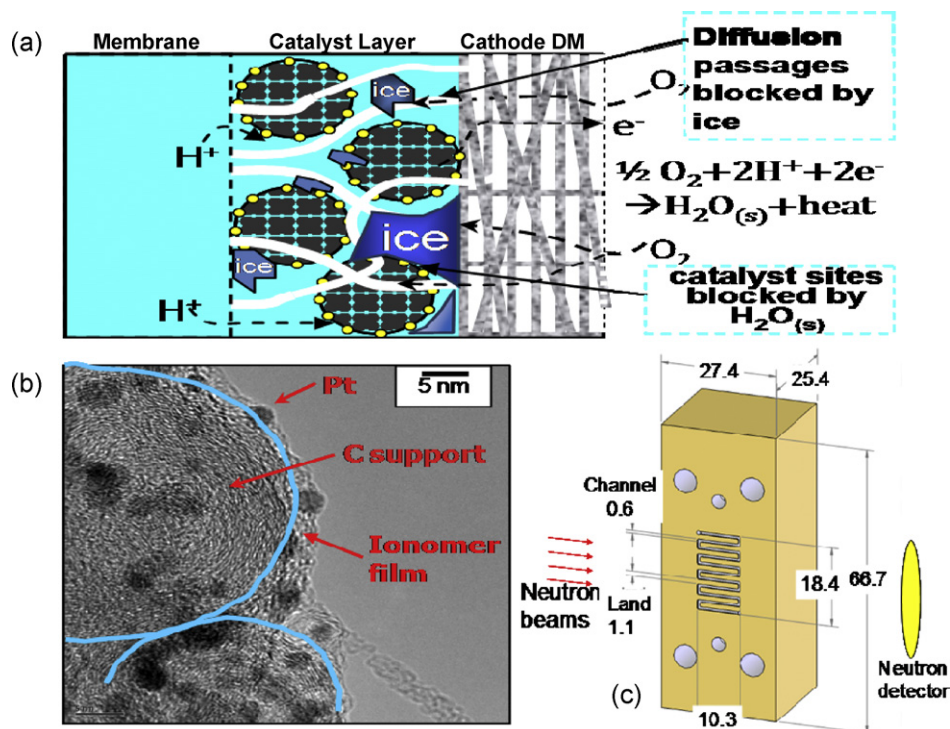


**Fig. 1.** Schematic of ice formation during fuel cell subfreezing operation (a); TEM of the catalyst layer surface (b); and the flow field design of the experimental PEFC for the neutron imaging studies (the unit: mm) (c).

Neutron imaging has been developed as a powerful tool for *in situ* measurements of the water content in fuel cells [22–28]. Owejan et al. [22,25] studied the water content in flow fields. Hickner et al. [26] measured the water distributions at operating conditions. Wang et al. [16] presented the water accumulations under channels and lands, respectively, for two subfreezing temperatures. Kramer and Zhang [27] investigated the liquid flow in flow fields and GDLs. Recently, a new detector technology based on micro-channel plates was installed at the NIST neutron facility [28], enabling higher resolution water detection.

Although a significant amount of effort has been made, several key aspects of cold start are still lacking and require further investigation. For example, most model predictions have not been validated yet. The location of ice formation is not fully understood and direct experimental visualizations are scarce. Few studies have addressed durability issues in freeze/thaw cycling. In this paper, several relevant aspects of fuel cell cold start are investigated. We first employ high-resolution neutron radiography to investigate ice location. Then the spatial variation of the reaction rate is discussed under subfreezing temperatures through evaluating a dimensionless parameter  $\bar{h}$  using newly developed membrane ionic conductivity. By identifying the operating range that the reaction can be treated uniform across the catalyst layer in which the model is valid, we compared the model prediction with experimental data. Because of ice formation in the cathode and the high value the ice volume fraction can reach during cold start, cold start can affect catalyst layer durability. We also briefly examine the loss of the active catalyst surface area.

## 2. Experimental

Experiments were conducted on laboratory-scale fuel cells with a 50 cm<sup>2</sup> active area, and on neutron imaging-scale fuel cells with a 2.5 cm<sup>2</sup> active area. Various MEAs and GDLs were considered, as summarized in Table 1. The 50 cm<sup>2</sup> fuel cells had quad-serpentine

flow fields, while the 2.5 cm<sup>2</sup> fuel cells had a single-serpentine flow field.

The fuel cells were first operated at 80 °C and a specified relative humidity (RH) at moderate current density, then shut down and purged with nitrogen at 2–5 L/min for 0.5–5 min. The temperature was then reduced to subzero using coolant flows. While at subzero temperature, the fuel cells were operated isothermally by applying a constant current at high stoichiometries until operation failure. Both high frequency resistance (HFR) and voltage evolution were measured. While operating under the above-described conditions, the 2.5 cm<sup>2</sup> fuel cells were imaged using the thermal beam line #2 neutron imaging facility at the NIST Center for Neutron Research (NCNR). Neutron radiographs were taken using the microchannel plate detector with a per-pixel spatial resolution of ~15 μm. The exposure time is 1 min. An example of neutron images is shown in Fig. 2(a) and (b), which clearly shows the MEA location, the middle bright region, because of ice production and accumulation. Fig. 2(c) presents the ice content profiles obtained through neutron imaging. The profiles were obtained by comparing dry and wet images

**Table 1**  
MEAs and GDLs used in the experiment.

Components	Material configuration
MEA	Homemade ELAT decal-transfer MEA (0.2 mg/cm <sup>2</sup> Pt on Vulcan XC-72 carbon) Gore Primea
	Nafion® 212 (50 μm, 0.2/0.2 mg Pt cm <sup>-2</sup> anode/cathode) MESGA® (18 μm, 0.1/0.2 mg Pt cm <sup>-2</sup> anode/cathode)
GDL	E-Tek ELAT cloth GDL
	SGL low PTFE Paper GDL
	SGL high PTFE paper GDL
	Double sided (cathode), single sided (anode) 24 B''C'' (5% PTFE in substrate and 5% PTFE in MPL) 24 B''C'' (5% PTFE in substrate and 23% PTFE in MPL)

Download English Version:

<https://daneshyari.com/en/article/188847>

Download Persian Version:

<https://daneshyari.com/article/188847>

[Daneshyari.com](https://daneshyari.com)